MEDICAL SCIENCE MONITOR

CLINICAL RESEARCH

e-ISSN 1643-3750
© Med Sci Monit, 2019; 25: 6351-6358
DOI: 10.12659/MSM.916112

Received: 2019.03.08
Accepted: 2019.04.08
Published: 2019.08.24

Micro-Computed Tomography (Micro-CT) Evaluation of Effects of Different Rotary Glide Path Techniques on Canal Transportation and Centering in Curved Root Canals

Authors' Contribution:
Study Design A
Data Collection B
Statistical Analysis C
Data Interpretation D
Manuscript Preparation E
Literature Search F
Funds Collection G

ABCDEF 1 Gabrielė Česaitienė
ADEG 1 Tadas Venskutonis
EG 1 Vita Mačiulskienė
BCDE 2 Vaidotas Cicėnas
BCDE 2 Vykintas Samaitis
BCDEG 2,3 Elena Jasiūnienė

1 Department of Dental and Oral Pathology, Lithuanian University of Health Sciences, Kaunas, Lithuania
2 Prof. K. Baršauskas Ultrasound Research Institute, Kaunas University of Technology, Kaunas, Lithuania
3 Department of Electronics Engineering, Kaunas University of Technology, Kaunas, Lithuania

Corresponding Author: Tadas Venskutonis, e-mail: Tadasvens@gmail.com
Source of support: The research leading to these results received funding from the Kaunas University of Technology and Lithuanian University of Health Sciences under grant agreement Nr. MTEPI-L-16014, project MEICENTRANSP, "Comparison of root canal transportation and centering ability of rotary endodontics instruments with constant and variable tapper, using X-ray micro-tomography"

Background: The aim of this study was to evaluate the ability of different rotary glide path techniques to maintain canal anatomy by comparing canal transportation and centring abilities in curved root canals using X-ray micro-computed tomography (micro-CT).

Material/Methods: We selected 36 root canals and randomly assigned them to 3 groups. The first group was instrumented using Pathfile (PF) 1 and PF2, the second group using PF2, and the third group using a Proglider (PG) instrument. Selected tooth samples were scanned using a micro-CT system with 8-µm resolution. Centring ability and transportation were compared at 5 levels: 0.5 mm (A0) and 1 mm (A1) from apical foramen, at the point of maximum root curvature (C0), at 1 mm below it (C–), and 1 mm above it (C+). Area, ratio of areas (RA), perimeter, centroid shift, mean diameter, and ratio of diameter ratios (RDR) were assessed.

Results: In all groups, there were no significant differences between different levels in all parameters (p>0.05). In group 1, the centroid shift was greatest at A0 and C–, and the least impact was at C0. In group 2, the biggest impacts were at C– and A0, and the smallest at C+. In group 3, the greatest impacts were at A0 and A1, and the smallest at C0.

Conclusions: All 3 instrument groups performed very similarly, without significant differences in canal-shaping parameters. Overall, using just PF2 instead of PF 1 and 2 created very similar shaping results, which could reduce the number of instruments needed and the cost of treatment.

MeSH Keywords: Endodontics • Root Canal Preparation • X-Ray Microtomography

Full-text PDF: https://www.medscimonit.com/abstract/index/idArt/916112

Indexed in: [Current Contents/Clinical Medicine] [SCI Expanded] [ISI Alerting System] [ISI Journals Master List] [Index Medicus/MEDLINE] [EMBASE/Excerpta Medica] [Chemical Abstracts/CAS]

Background

The main goals of mechanical root canal preparation are to remove vital or necrotic pulp tissues, eliminate infected dentin, and prepare space for disinfection agents and filling materials [1]. Glide path creation facilitates cleaning and shaping processes in curved root canals [2]. Most root canals are curved on 1 or more planes and have irregular canal cross-sections, while instruments are manufactured from thin, straight, metal wires [3–5]. Instruments tend to straighten in the root canal [6] and this results in asymmetrical dentine removal during shaping, leading to canal transportation [3,5,7–10]. There are various methods used in clinical practice for rotary glide path preparation: PathFiles (PF, Dentsply Sirona, USA), Proglider (PG, Dentsply Sirona, USA), Race ISO 10 (FKG, Switzerland), ScoutRace (FKG, Switzerland), One G (Micro – Mega, France), EdgeGlidePath (EdgeEndo, New Mexico), WaveOne Gold Glider (Dentsply Sirona, USA), and R-pilot (VDW, Germany) [11]. The PF system is manufactured from regular nickel-titanium wire and consists of 3 instruments with tip sizes of ISO PF1–0.13 mm, PF2–0.16 mm, and PF3–0.19 mm and a fixed 2% taper. PG instruments are manufactured from heat-treated M-wire with ISO 0.16 mm tip size and a 2% to 8% progressive taper [12].

X-ray micro-computed tomography (micro-CT) is used more and more often for the investigation of root canals because it allows detailed, non-destructive, 3-dimensional (3D) analysis of the root canals [4,13–15], enabling evaluation of the shaping properties of different instruments at selected levels before and after endodontic preparation [16–25]. Various parameters can be evaluated, such as the volume of the root canal [26–30], area, perimeter [6,27,28], and diameter changes [20] in different slices before and after instrumentation [7,17,26].

Clinicians often use modified glide path preparation techniques using PF1 and PF2 or just PF2 [31]. The objective of this study was to evaluate the impact of different glide path techniques, all ending with ISO 0.16-mm tip instruments, on canal transportation and centering in curved root canals using micro-CT. The first sequence in the present study was recommended by the manufacturer, and only the PF2 instrument was used in the second sequence.

Material and Methods

Selection of teeth

For this study, mesiobuccal and distobuccal canals of upper molars and mesiobuccal and mesiolingual canals of lower molars were selected. All teeth were extracted because of irreparable tooth damage due to severe crown decay, non-treated apical and marginal periodontitis, or orthodontic reasons. The main inclusion criteria were narrow, previously untreated, separate (type I and IV Vertucci classification) canals with closed apices and curvatures of 25° to 30° [32]. Curvatures were determined by using the Schneider technique [33]. A total of 36 teeth met inclusion criteria. The pulp chamber was opened and canal orifices were located with the aid of a dental microscope (M320, Leica Microsystem, DB). The passage of the canals was checked using a 0.06 K-File (Dentsply Sirona, USA). Roots were separated from the crown with a 0.15-mm thickness diamond disc (Edenta, Switzerland) and kept in saline solution. The Local Ethics Committee approved the study.

Micro-CT analysis

The selected tooth samples were fixed on custom-made, stable holders to ensure the same positioning before and after the instrumentation. The samples were scanned using the X-ray 3D Computer tomography system RayScan 250E (RayScan Technologies GmbH, Meersburg, Germany). The measurements were carried out using a 10-230 kV micro focus X-ray source. A flat panel detector measuring 2048×2048 pixels was used. Overall, 2520 projections were acquired with a 1 s integration time, averaging 3 at a 90 kV voltage and 90 µA current, with a resulting voxel size of 8 µm.

Specimen preparation

Thirty-six root canals were selected and randomly assigned to 3 groups (n=12). The canals were instrumented using a 0.08, 0.10 K-File (Dentsply Sirona, USA). Working length was controlled and measured with the aid of the dental microscope.

The groups were as follows:
- Group 1 was instrumented using PF1 and PF2 instruments,
- Group 2 was instrumented using a PF2 instrument,
- Group 3 was instrumented using a PG instrument.

The rotary instrument was controlled with an X-Smart plus motor (Dentsply Sirona, USA) using 2.0 N torque with a speed of 300 rpm. During and after instrumentation, the canals were irrigated using 2.5% sodium hypochlorite.

Micro-CT scanning and 3D analysis

Each tooth specimen was scanned twice: the first scan was performed before any intervention to the root canal, and the second one was performed after the cleaning sequence by K-file and glide path instruments. Data analysis was performed in 2 stages. During the first stage, reconstruction of the root canal central line was performed in 3D and images of 5 cross-sections were produced orthogonal to the canal in order to evaluate the impact of different glide path techniques. For the first stage, reconstruction of the root canal cavity center line and

Indexed in: [Current Contents/Clinical Medicine] [SCI Expanded] [ISI Alerting System] [ISI Journals Master List] [Index Medicus/MEDLINE] [EMBASE/Excerpta Medica] [Chemical Abstracts/CAS]

the root canal volume was reconstructed using Avizo Inspect (FEI, France) software. The next step was slicing the root canal volume by perpendicular planes and calculation of the mass center point for each slice. All points were then joined by lines and smoothed using approximation. The root center point array coordinates were exported to MATLAB and the curvature of the root was calculated.

For the angle calculation of the canal center line, the length of the standard line, which will be used as the reference line, has to be considered. The short reference line is sensitive to random noise; on the other hand, the longer line's integration capability is higher and small curvature variations can be lost. It was determined that a reasonable compromise between filtering the noise and preservation of sensitivity is about 1/10 of the overall root canal length *n*. For this research, a length of standard line of Δk=1 mm was selected for all samples.

The first point *C(1)* from the center line data set *C(1,2,..,n)* was connected with the point *C(i)*, which is closest to the standard line length Δk. The most distant point *M(j)* from array *C(1,2,..,i)* to the line *L(1,i+ Δk)* was calculated; this point is the intersection point of 2 straight lines drawn trough the points *C(i)*, *M(j)* and points *C(i+Δk)*, *M(j* (Figure 1A).

The angle between these 2 straight lines in 3D space can be calculated by the following expression:

$$\propto (\mathrm{i}) = \arccos\left(\frac{\overrightarrow{C_1M_J}\cdot\overrightarrow{C_{1+\Delta k}M_J}}{\|\overrightarrow{C_1M_J}\|\|\overrightarrow{C_{1+\Delta k}M_J}\|}\right) - \frac{\pi}{2},$$

The calculated maximum angle value is assigned to the array, which describes the curvature of tooth root canal center line.

Five specific points on the center line were then calculated:
- Point A0, 0.5 mm from the apical towards crown,
- Point A1, 1 mm from the apical towards crown,
- Point C0, point of the maximum curvature of the root canal,
- Point C–, 0.5 mm from point C0 towards apical,
- Point C+, 0.5 mm from point C0 towards crown.

The root cross-sectional slice images at these points perpendicular to the root center line were produced (Figure 1B). The cross-sectional slice image set consisted of 5 images made before and 5 images made after the instrumentation at the previously described specific points for each sample.

2D analysis

Second-stage analysis included the calculation of the 2D parameters at 5 root-canal-specific sections orthogonal to the canal axis. A special algorithm for root canal geometrical analysis was developed, which compared various root canal parameters at a given cross-section before and after preparation from the projection images. The examples of input cross-sectional images are presented in Figure 2.

The algorithm analyses the root canal region within the selected window. The root canal cross-sectional images are then converted to a binary format and the following parameters are estimated:

Area: number of pixels in the selected cluster before and after preparation:

$$A_{\mathrm{pre}} = A_{\mathrm{pre}_0}\cdot\sum_{k=1}^{K} I_{\mathrm{pre}}(x_k, y_k),\quad A_{\mathrm{post}} = A_{\mathrm{post}_0}\cdot\sum_{k=1}^{K} I_{\mathrm{post}}(x_k, y_k), \qquad (1)$$

where $(x_k,y_k)\in$ ROI, K is the number of pixels in the analysed area, I_{pre}, I_{post} is the binary image of the root canal before and after preparation, respectively, A_{pre0}, A_{post0} is the area of a single pixel before and after preparation (voxel size).

The percentage change in root canal area is estimated:

$$A_{\%} = 100\% - \frac{A_{\mathrm{pre}}\cdot 100\%}{A_{\mathrm{post}}}. \qquad (2)$$

Ratio of areas (RA):

$$\mathrm{RA} = \frac{A_{\mathrm{post}}}{A_{\mathrm{pre}}}, \qquad (3)$$

where A_{post} and, A_{pre} are the post-preparation and pre-preparation cross-sectional areas. Values close to 1 correspond to little difference between the *post*- and *pre*-instrumentation measurements.

Perimeter: length of the detected root canal boundary.

$$P = \sum_{i=1}^{N} p_i, \qquad (4)$$

$$p_i = \sqrt{(x_i - x_{i+1})^2 + (y_i - y_{i+1})^2},\quad p_N = \sqrt{(x_N - x_1)^2 + (y_N - y_1)^2}, \qquad (5)$$

where i=1÷N–1, N is the number of points which lie on the boundary of root canal, (x_i,y_i) is the coordinates of the pixels, located on the boundary of the root canal.

The percentage change in root canal perimeter is estimated:

$$P_{\%} = 100\% - \frac{P_{\mathrm{pre}}\cdot 100\%}{P_{\mathrm{post}}}. \qquad (6)$$

where P_{post} and, P_{pre} are the post-preparation and pre-preparation perimeters.

Coordinates of centroid:

$$x_c = \frac{1}{K}\sum x_k,\quad y_c = \frac{1}{K}\sum y_k, \qquad (7)$$

Indexed in: [Current Contents/Clinical Medicine] [SCI Expanded] [ISI Alerting System] [ISI Journals Master List] [Index Medicus/MEDLINE] [EMBASE/Excerpta Medica] [Chemical Abstracts/CAS]

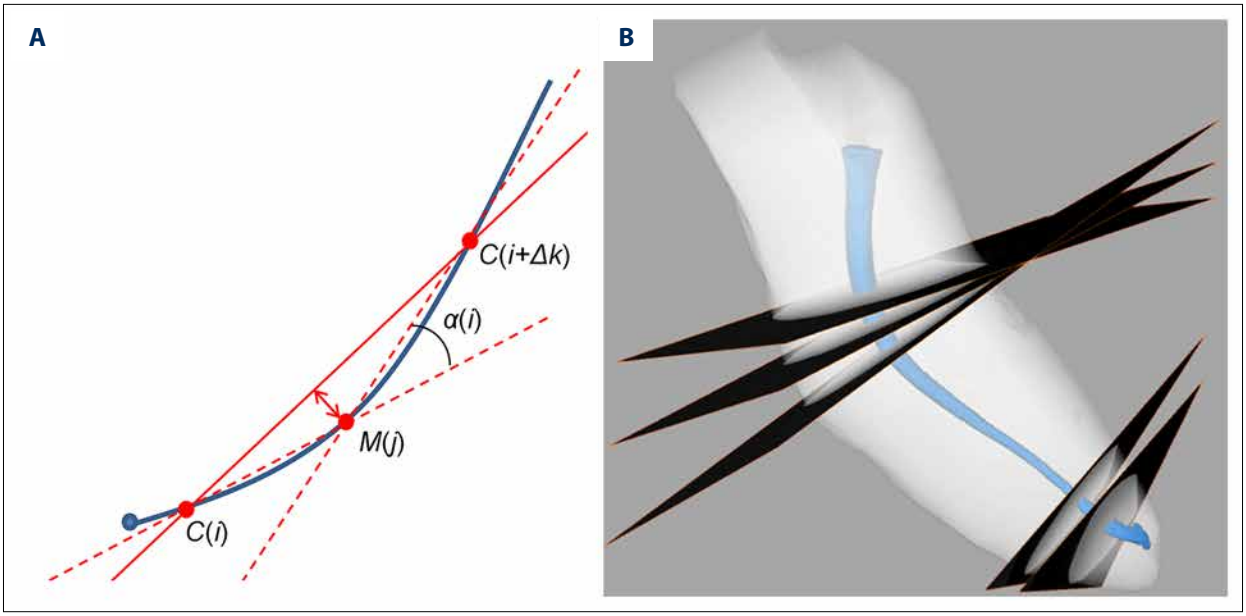

Figure 1. The center line curvature calculation of the root canal (**A**) and 5 cross-section planes orthogonal to the canal axis (**B**) (from the top: C+, C0, C–, A1, A0).

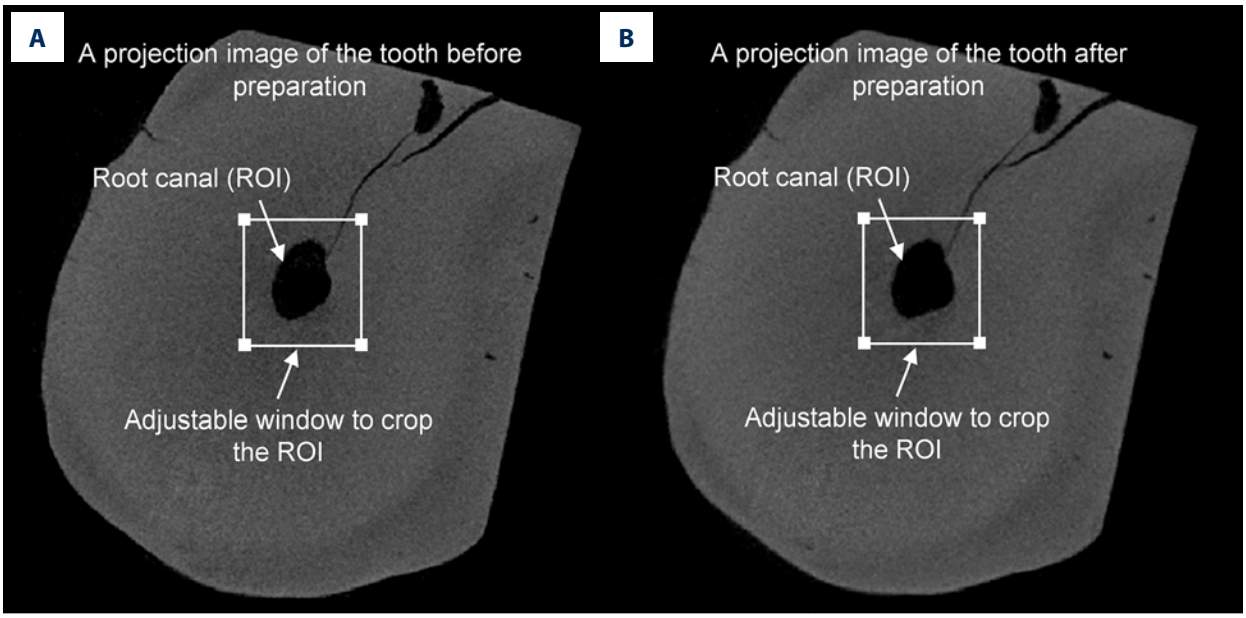

Figure 2. The projection images of the tooth before (**A**) and after (**B**) preparation, which were used as input data during the analysis.

Shift of centroid: Centroid shift after canal preparation in respect to the initial state.

$$\Delta m_c = \sqrt{\left(x_{c_{pre}} - x_{c_{post}}\right)^2 + \left(y_{c_{pre}} - y_{c_{post}}\right)^2}, \quad (8)$$

where indices "*pre*" and "*post*" denote the centroid coordinates before and after preparation, respectively.

Diameter: the distance between 2 points located at the opposite sides of the boundary of the cluster at each 1° increment.

$$R_i = \sqrt{(x_c - x_i)^2 + (y_c - y_i)^2}, \quad (9)$$

$$\alpha_m = \text{atan2}\left(\frac{y_i - y_c}{x_i - x_c}\right), \quad (10)$$

$$D_m = R_i(\alpha_m) - R_i(\alpha_m + \pi),\ \alpha_m \in [0 \div \pi] \quad (11)$$

where $\alpha m \in [0 \div \varpi]$, $m=1 \div M$, M is the number of considered angles.

Indexed in: [Current Contents/Clinical Medicine] [SCI Expanded] [ISI Alerting System] [ISI Journals Master List] [Index Medicus/MEDLINE] [EMBASE/Excerpta Medica] [Chemical Abstracts/CAS]

Mean diameter:

$$D_{\Sigma_{pre}} = \frac{\sum_{i=1}^{m} D_{m_{pre}}}{m},\ D_{\Sigma_{post}} = \frac{\sum_{i=1}^{m} D_{m_{post}}}{m}, \quad (12)$$

$$D_{\%} = 100\% - \frac{D_{\Sigma_{pre}} \cdot 100\%}{D_{\Sigma_{post}}}, \quad (13)$$

where $D_{\Sigma pre}$, $D_{\Sigma post}$ is the mean diameter before and after preparation.

Ratio of diameter ratios (RDR):

$$RDR = \frac{\left(D_{post} / d_{post}\right)}{\left(D_{pre} / d_{pre}\right)}, \quad (14)$$

where (D_{post}/d_{post}) is the post-preparation ratio of the major diameter D_{post} and minor diameter d_{post} (D_{post}=max(D_{mpost}), d_{post}=min(D_{mpost})), (D_{pre}/d_{pre}) is the pre-preparation ratio of D_{pre} to d_{pre}. The graphical illustration of the analysed parameters is presented in Figure 3.

Statistical analysis

The statistical analysis was performed with SPSS software version 19.0 (SPSS, Inc, Chicago, IL). Significance was set at a P value of 0.05 or less. All parametric data were expressed as the mean and standard deviation (SD) or the mean and 95% confidence interval. Chi-square tests were used to compare the frequencies of qualitative variables. A Kolmogorov-Smirnov test was used for determination of quantitative data distribution. When the distribution of variables was normal, a one-way analysis of variance (ANOVA) was used to compare instruments. A Kruskal-Wallis test was used to compare non-normally distributed variables.

Results

All 6 parameters (area, diameter, perimeter, RDR, RA, and centroid shift) were analyzed by comparing data from each group between different levels of analysis (A0, A1, C+, C–, C0). Different instrument groups were also compared when all levels of canal were combined. All the data can be seen in Table 1.

In groups 1, 2, and 3, there were no significant differences between different levels in all parameters (p>0.05). In group 1, centroid shift was biggest at A0 and C–, and the least impact was at C0. In group 2, the biggest impacts were at C– and A0, and the smallest at C+. In group 3, the biggest impacts were at A0 and A1, with the smallest at C0. The worst RDR score was in level A0 (group 1 and 2) and A1 (group 3), indicating more asymmetrical preparation in these regions.

In comparing different groups with all 6 levels combined, there were no statistically significant differences between them in any parameters P>0.05. The biggest increase in canal diameter was for group 1 instruments. The values of RA were closer to 1 for groups 2 and 3. The RDR score for group 2 was closer to 1, resulting in more symmetrical preparation.

Discussion

Various studies have investigated the ability of different endodontic instruments to maintain original canal anatomy. Most studies have compared rotary root canal preparation with manual preparation [18,34–37] or reciprocating preparation [36–38]. Also, many studies have evaluated shaping instruments' ability to adjust in narrow and curved canals [12,17,39], but only a few studies compared glide path instruments [18,20,35,37]. There have been no studies comparing 2 sequences of PF instruments with PG instruments. The first sequence in the present study was recommended by the manufacturer, and the second sequence suggests using only a PF2 instrument.

Pasqualini et al. and found that NiTi alloy PF instruments (used with the manufacturer's recommended sequence) can preserve the original canal anatomy better than stainless steel hand files [35]. Paleker et al. suggested that PG instruments were also more centered and caused less transportation than manual preparation [18]. Post shaping analysis in a study by Alovisi et al. demonstrated that the PG instrument's ability to center the root canal is the same as with PF instruments [20]. In agreement with the above, the present study showed that PG instruments caused more canal centroid shift in the apical area than both sequences of PF instruments (without significant difference, P>0.05). The PF 2 led to a bigger centroid shift in the apical part, and less in the upper part of the canals, than using both PF1 and PF2 (without significant difference, P>0.05). The RDR and RA also corresponded to that reported in the Alovisi et al. study, with no differences between groups [20].

In all 3 groups, the biggest centroid shift was at the level of 0.5 mm from the apical part (but without significant difference, P>0.05).

In this study, there was no difference in area and perimeter increase between all groups, which is in agreement with Kirchhoff et al. [12]. In contrast, Alovisi et al. found that PG instruments significantly increase volume and area [20]. This difference could be due to the different reference points inside the canal; PG is more tapered, so if we look closer to the orifice, the PG instrument may produce more transportation and enlargement.

Computed tomography allows a detailed 3D investigation of root canal anatomy and different parameters [40]. Junaid et al.

Indexed in: [Current Contents/Clinical Medicine] [SCI Expanded] [ISI Alerting System] [ISI Journals Master List] [Index Medicus/MEDLINE] [EMBASE/Excerpta Medica] [Chemical Abstracts/CAS]

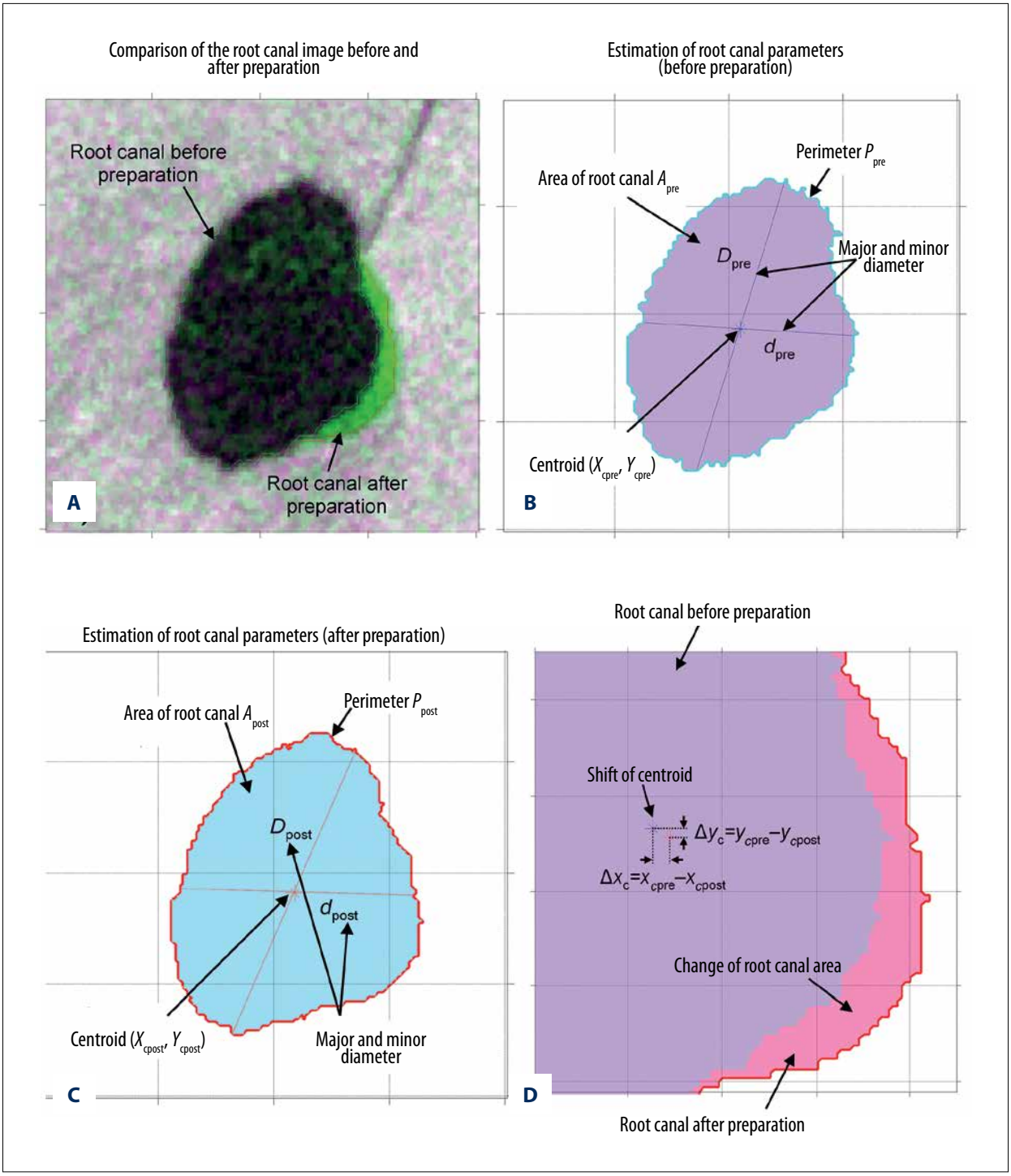

Figure 3. Graphical illustration of the analyzed root canal parameters: comparison of root canal geometry before and after preparation (**A**), estimated root canal parameters before preparation (**B**), estimated root canal parameters after preparation (**C**), shift of centroid and change in area due to preparation (**D**).

Indexed in: [Current Contents/Clinical Medicine] [SCI Expanded] [ISI Alerting System] [ISI Journals Master List] [Index Medicus/MEDLINE] [EMBASE/Excerpta Medica] [Chemical Abstracts/CAS]

Table 1. Mean changes including standard deviation of the evaluated parameters and their significances value.

Level of analysis		Area difference, mm²	Diameter difference, µm	Perimeter difference, µm	RDR	RA	Centroid shift, µm
Group 1	A0	0.004±0.007	14±25	54±109	0.91±0.27	1.25±0.48	7.9±4.7
	A1	0.006±0.007	18±25	30±123	0.94±0.08	1.27±0.45	6.8±3.9
	C+	0.006±0.008	17±27	108±405	0.91±0.14	1.26±0.55	6.9±3.1
	C–	0.005±0.007	15±25	169±606	0.98±0.09	1.19±0.48	7.4±3.1
	C0	0.005±0.007	12±20	23±187	1.01±0.05	1.15±0.32	6.7±3.1
	Overall	0.005±0.007	15±24	43±341	0.95±0.15	1.22±0.45	7.1±3.5
P Inside group 1		**0.98**	**0.98**	**0.57**	**0.51**	**0.97**	**0.94**
Group 2	A0	0.004±0.002	12±6	21±112	0.93±0.10	1.11±0.08	8.1±4.3
	A1	0.004±0.005	9±10	16±103	0.97±0.08	1.06±0.10	6.9±4.5
	C+	0.003±0.004	6±9	55±162	0.99±0.04	1.03±0.07	5.6±4.5
	C–	0.005±0.004	9±8	92±233	0.95±0.11	1.06±0.10	9.0±9.1
	C0	0.005±0.005	10±11	63±155	0.96±0.08	1.08±0.12	5.7±4.5
	Overall	0.004±0.004	9±9	49±157	0.96±0.08	1.07±0.09	7.1±5.7
P Inside group 2		**0.68**	**0.53**	**0.76**	**0.55**	**0.42**	**0.51**
Group 3	A0	0.004±0.005	12±17	48±117	0.93±0.20	1.09±0.12	8.8±7.2
	A1	0.004±0.007	12±19	59±181	0.88±0.19	1.09±0.14	8.7±7.5
	C+	0.004±0.013	5±11	159±274	0.99±0.04	1.02±0.03	7.5±5.3
	C–	0.005±0.006	7±8	299±480	0.98±0.07	1.01±0.02	5.3±3.3
	C0	0.007±0.014	7±12	179±225	0.96±0.05	1.02±0.03	5.0±2.8
	Overall	0.005±0.009	8±14	149±288	0.95±0.13	1.04±0.09	7.1±5.6
P Inside group 3		**0.94**	**0.68**	**0.24**	**0.34**	**0.09**	**0.34**
P between the groups		**>0.05**	**>0.05**	**>0.05**	**>0.05**	**>0.05**	**>0.05**

SD – standard deviation; P – significance value; RDR – ratio of diameter ratios; RA – ratio of areas.

reached 35 µm resolution [19], Leoni et al. reached 22.9 µm [41], and De-Deus et al. reached 14.5 µm [42]. One of the main goals of our study was to reach the highest possible resolution images of CBCT, because very thin (with 0.16-mm tip) instruments were used for glide path creation. In this study, the voxel size of 3D views was 8 µm.

Conclusions

Creating a glide path is the first step of root canal treatment, and further shaping depends on a successful start. All 3 instrument groups performed very similarly, without significant differences in canal-shaping parameters. This study has shown that using 2 instruments (Group 1) created a bigger centroid shift than using only 1 instrument (Groups 2, 3). Overall, using just the PF2 instead of the PF1 and PF2 created very similar shaping results. A proposed modified PF sequence using only the PF2 instrument could be used in clinical practice without a significant difference in canal transportation parameters. These findings could enable the reduction of the number of instruments used and reduce the cost of the treatment. Of course, the load on the instruments is greater in that case, which needs to be further investigated.

Conflicts of interest

None.

Indexed in: [Current Contents/Clinical Medicine] [SCI Expanded] [ISI Alerting System] [ISI Journals Master List] [Index Medicus/MEDLINE] [EMBASE/Excerpta Medica] [Chemical Abstracts/CAS]

References:

1. Hülsmann M, Peters OA, Dummer PMH: Mechanical preparation of root canals: Shaping goals, techniques and means. Endod Topics, 2005; 10: 30–76
2. Adıgüzel M, Yılmaz K, Tüfenkçi P: Comparison of postoperative pain intensity after using reciprocating and continuous rotary glide path systems: A randomized clinical trial. Restor Dent Endod, 2019; 44: e9
3. Peters OA: Current challenges and concepts in the preparation of root canal systems: A review. J Endod, 2004; 30: 559–67
4. Lee JK, Ha BH, Choi JH et al: Quantitative three-dimensional analysis of root canal curvature in maxillary first molars using micro-computed tomography. J Endod, 2006; 32: 941–45
5. Peters OA, Laib A, Rüegsegger P, Barbakow F: Three-dimensional analysis of root canal geometry by high-resolution computed tomography. J Dent Res, 2000; 79: 1405–9
6. Marceliano-Alves MFV, Sousa-Neto MD, Fidel SR et al: Shaping ability of single-file reciprocating and heat-treated multifile rotary systems: A micro-CT study. Int Endod J, 2014; 48: 1129–36
7. Moore J, Fitz-Walter P, Parashos P: A micro-computed tomographic evaluation of apical root canal preparation using three instrumentation techniques. Int Endod J, 2009; 42: 1057–64
8. Bürklein S, Hinschitza K, Dammaschke T, Schäfer E: Shaping ability and cleaning effectiveness of two single-file systems in severely curved root canals of extracted teeth: Reciproc and WaveOne versus Mtwo and ProTaper. Int Endod J, 2012; 45: 449–61
9. Bürklein S, Mathey D, Schäfer E: Shaping ability of ProTaper NEXT and BT-RaCe nickel-titanium instruments in severely curved root canals. Int Endod J, 2015; 48: 774–81
10. Bürklein S, Jäger PG, Schäfer E: Apical transportation and canal straightening with different continuously tapered rotary file systems in severely curved root canals: F6 SkyTaper and OneShape versus Mtwo. Int Endod J, 2017; 50: 983–90
11. Cassim I, van der Vyver PJ: The importance of glide path preparation in endodontics: A consideration of instruments and literature. SADJ, 2013; 68: 322, 324–27
12. Kirchhoff AL, Chu R, Mello I et al: Glide path management with single- and multiple-instrument rotary systems in curved canals: A micro-computed tomographic study. J Endod, 2015; 41: 1880–83
13. Amoroso-Silva PA, Ordinola-Zapata R, Duarte MAH et al: Micro-computed tomographic analysis of mandibular second molars with C-shaped root canals. J Endod, 2015; 41: 890–95
14. Somma F, Leoni D, Plotino G et al: A Root canal morphology of the mesiobuccal root of maxillary first molars: A micro-computed tomographic analysis. Int Endod J, 2009; 42: 165–74
15. Paqué F, Barbakow F, Peters OA: Root canal preparation with Endo-Eze AET: Changes in root canal shape assessed by micro-computed tomography. Int Endod J, 2005; 38: 456–64
16. Fan B, Yang J, Gutmann JL, Fan M: Root canal systems in mandibular first premolars with C-shaped root configurations, Part I: Microcomputed tomography mapping of the radicular groove and associated root canal cross-sections. J Endod, 2008; 34: 1337–41
17. Pasqualini D, Alovisi M, Cemenasco A et al: Micro-computed tomography evaluation of protaper next and biorace shaping outcomes in maxillary first molar curved canals. J Endod, 2015; 41: 1706–10
18. Paleker F, van der Vyver PJ: Comparison of canal transportation and centering ability of K-files, ProGlider file, and G-files: A micro-computed tomography study of curved root canals. J Endod, 2016; 42: 1105–9
19. Junaid A Freire, LG, da Silveira Bueno CE et al: Influence of single-file endodontics on apical transportation in curved root canals: An *ex vivo* micro-computed tomographic study. J Endod, 2014; 40: 717–20
20. Alovisi M, Cemenasco A, Mancini L et al: Micro-CT evaluation of several glide path techniques and ProTaper Next shaping outcomes in maxillary first molar curved canals. Int Endod J, 2017; 50: 387–97
21. Peters OA, Schonenberger K, Laib A: Effects of four Ni-Ti preparation techniques on root canal geometry assessed by micro computed tomography. Int Endod J, 2001; 34: 221–30
22. Bergmans L, Van Cleynenbreugel J, Wevers M, Lambrechts P: A methodology for quantitative evaluation of root canal instrumentation using micro-computed tomography. Int Endod J, 2001; 34: 390–98
23. Peters OA, Peters CI, Schonenberger K, Barbakow F: ProTaper rotary root canal preparation: Effects of canal anatomy on final shape analysed by micro CT. Int Endod J, 2003; 36: 86–92
24. Saberi N, Patel S, Mannocci F: Comparison of centring ability and transportation between four nickel titanium instrumentation techniques by micro-computed tomography. Int Endod J, 2017; 50: 595–603
25. Stern S, Pate, S, Foschi F et al: Changes in centring and shaping ability using three nickel-titanium instrumentation techniques analysed by micro-computed tomography (μCT). Int Endod J, 2012; 45: 514–23
26. Neves AA, Silva EJ, Roter JM et al: Exploiting the potential of free software to evaluate root canal biomechanical preparation outcomes through micro-CT images. Int Endod J, 2015; 48: 1033–42
27. Versiani MA, Pécora JD, Sousa-Neto MD: Microcomputed tomography analysis of the root canal morphology of single-rooted mandibular canines. Int Endod J, 2013; 46: 800–7
28. Pinheiro SR, Alcalde MP, Vivacqua-Gomes N et al: Evaluation of apical transportation and centring ability of five thermally treated NiTi rotary systems. Int Endod J, 2018; 51: 705–31
29. Silva EJNL, Pacheco PT, Pires F et al: Microcomputed tomographic evaluation of canal transportation and centring ability of ProTaper Next and Twisted File Adaptive systems. Int Endod J, 2017; 50: 694–99
30. Zuolo ML, Zaia AA, Belladonna FG et al: Micro-CT assessment of the shaping ability of four root canal instrumentation systems in oval-shaped canals. Int Endod J, 2018; 51: 564–71
31. Can EDB, Gerek M, Kayahan MB et al: Comparision of two different preparation protocol of Ni-Ti Rotary PathFile-ProTaper instruments in simulated s-shaped canals. Acta Odontol Scand, 2014; 72: 76–80
32. Vertucci FJ, Gegauff A: Root canal morphology and its relationship to endodontic procedures. J Am Dent Assoc, 1979; 99(2): 194–98
33. Schneider SW: A comparison of canal preparations in straight and curved root canals. Oral Surg Oral Med Oral Pathol, 1971; 32: 271–75
34. Paqué F, Ganahl D, Peters OA: Effects of root canal preparation on apical geometry assessed by micro-computed tomography. J Endod, 2009; 35: 1056–59
35. Pasqualini D, Bianchi CC, Paolino DS et al: Computed micro-tomographic evaluation of glide path with nickel-titanium rotary PathFile in maxillary first molars curved canals. J Endod, 2012; 38: 389–93
36. Zanesco C, Só MVR, Schmidt S et al: Apical transportation, centering ratio, and volume increase after manual, rotary, and reciprocating instrumentation in curved root canals: Analysis by micro-computed tomographic and digital subtraction radiography. J Endod, 2017; 43: 486–90
37. Prabhakar AR, Yavagal C, Dixit K, Naik SV: Reciprocating vs rotary instrumentation in pediatric endodontics: Cone beam computed tomographic analysis of deciduous root canals using two single-file systems. Int J Clin Pediatr Dent, 2016; 9: 45–49
38. Hoppe CB, Böttcher DE, Just AM et al: Comparison of curved root canals preparation using reciprocating, continuous and an association of motions. Scanning, 2016; 38: 462–68
39. Shah DY, Wadekar SI, Dadpe AM et al: Canal transportation and centering ability of protaper and self-adjusting file system in long oval canals: An *ex-vivo* cone-beam computed tomography analysis. J Conserv Dent, 2017; 20: 105–9
40. Kim H-C, Lee MH, Yum J et al: Potential relationship between design of nickel-titanium rotary instruments and vertical root fracture. J Endod, 2010; 36: 1195–99
41. Leoni GB, Versiani MA, Pécora JD, Damião de Sousa-Neto M: Micro-computed tomographic analysis of the root canal morphology of mandibular incisors. J Endod, 2014; 40: 710–16
42. De-Deus G, Belladonna FG, Souza EM et al: Micro-computed tomographic assessment on the effect of ProTaper next and twisted file adaptive systems on dentinal cracks. J Endod, 2015; 41: 1116–19

Indexed in: [Current Contents/Clinical Medicine] [SCI Expanded] [ISI Alerting System] [ISI Journals Master List] [Index Medicus/MEDLINE] [EMBASE/Excerpta Medica] [Chemical Abstracts/CAS]